Contour Decouples Gamma Activity Across Texture Representation in Monkey Striate Cortex

Alexander Gail, Hans Joerg Brinksmeyer and Reinhard Eckhorn

Philipps-University, Physics Department, Neurophysics Group, Renthof 7, D-35032 Marburg, Germany

Previous work on figure–ground coding in monkey V1 revealed enhanced spike rates within an object's surface representation, synchronization of gamma oscillations (γ = 35–90 Hz) in object and background regions, but no decrease in signal correlation across the representation of a contour. The latter observation seems to contradict previous statements on the role of γ-synchronization for scene segmentation. We re-examine these findings by analyzing different coupling measures and frequency ranges of population activities potentially contributing to figure–ground segregation. Multiple unit activity (MUA) and local field potentials (LFPs) were recorded by parallel μ-electrodes in monkey V1 during stimulation by a grating in which an object was defined by a shifted rectangle. In contradiction to the conclusions in previous work, we find strong decoupling of population activity between figure and ground representations compared to the situation in which the object is absent. In particular, coherence of late γ-LFPs is strongly reduced, while reduction is absent during the early epochs of high-amplitude transients for LFP- and MUA-coherence at all frequencies, and at low frequencies also in the subsequent epochs. Our results of decoupling in late LFP γ-components among figure and ground representations suggest that these signals may support figure–ground segregation.

Introduction

Perceptual grouping and scene segmentation are basic aspects of early visual processing as has already been shown by Gestalt psychologists (Wertheimer, 1923; Koffka, 1935). These aspects are tightly connected to figure–ground segregation, a necessary requirement for object recognition. Segregation is a crucial and difficult task because the same object can appear on a variety of backgrounds, including the most difficult situation, which is composed of largely similar features for figure and ground. While many psychophysical investigations provide material about perceptual feature grouping in various visual situations [reviews in (Boucart, 1999)], neural mechanisms of figure–ground segregation are largely unknown.

Spike Rate Modulations for Figure–Ground Segregation

A classical approach to figure–ground segregation assumes convergent forward connections to a common target of those neurons representing the specific features of an object by their receptive fields. A small number of single cardinal neurons (Barlow, 1972) or a subgroup of neurons of an associative memory (Fukushima, 1980; Palm, 1982) may represent the presence of an object by an increase in their activation. Model investigations suggest an object-specific increase in spike rate, which in turn might suppress activities evoked by other objects via mutual or common feedback inhibition and thereby support segregation of figure from ground (Erb and Aertsen, 1993; Grossberg and Pessoa, 1998).

Object-specific increases in population spike rates (multiple unit activity, MUA) were indeed recently reported for neurons representing object surfaces relative to those representing background in monkey V1 (Lamme, 1995; Zipser *et al.*, 1996). Objects were defined by the contrast among textures consisting of the same elements inside and outside the object except for the value of one feature, as for example local line orientation. Object-specific rate increases disappeared under anesthesia, which was taken as indication of top-down influence (Lamme *et al.*, 1998a,b). Analysis of the temporal development of spike rate modulations suggested that figure–ground segregation may be initiated from the detection of contours, followed by the filling-in of the surfaces between these contours to render them visible (Lamme *et al.*, 1999).

Feature Grouping Based on Synchronized γ-Oscillations

Alternatively, figure–ground segregation may be based on the grouping of surface elements that are similar and adjacent, so that contours are identified as the borders between differing elements. This coding possibility is supported by the observation of cortical oscillations in the gamma range (35–90 Hz) in the visual cortex of cats (Eckhorn *et al.*, 1988; Gray *et al.*, 1989) and monkeys (Kreiter and Singer, 1992; Eckhorn *et al.*, 1993a) because they occur in several aspects according to Gestalt criteria of feature grouping [reviewed by a number of authors (Roelfsema *et al.*, 1996; Eckhorn, 1999; Gray, 1999)]. In this concept and related models, neurons representing features of the same object couple their activities transiently by forming synchronized assemblies (Eckhorn *et al.*, 1988, 1990; Gray *et al.*, 1989; Engel *et al.*, 1991a) [reviews in (Gray, 1999; Eckhorn, 1999)]. Segregation of figure from ground can in this concept either be coded by phase shifted (Horn *et al.*, 1991; Stoecker *et al.*, 1996) or decoupled γ-oscillations among object and background representations.

Contradictory Findings of Figure–Ground Segregation Based on Signal Decoupling

In one type of experiment, investigating scene segmentation, neurons with overlapping receptive fields of different orientation preferences were stimulated by either a single moving light bar or by a superposition of two light bars of different orientation and movement direction [cat V1 (Engel *et al.*, 1991a); monkey MT (Kreiter and Singer, 1996)]. While a single bar was reported to induce γ-oscillations that were coupled in many recordings, the two-bar situation reduced coupling and often generated two separate groups of neurons with internally correlated oscillations.

In a second type of experiment, neurons with separate receptive fields were recorded and stimulated either by a single moving stimulus (light bar or grating) or by two stimuli with a gap among them moving either in the same or in antagonistic directions [cat V1 (Gray *et al.*, 1989); V2 (Brosch *et al.*, 1997)]. For the single stimulus condition these studies also reported strongly correlated γ-oscillations for many of the activated

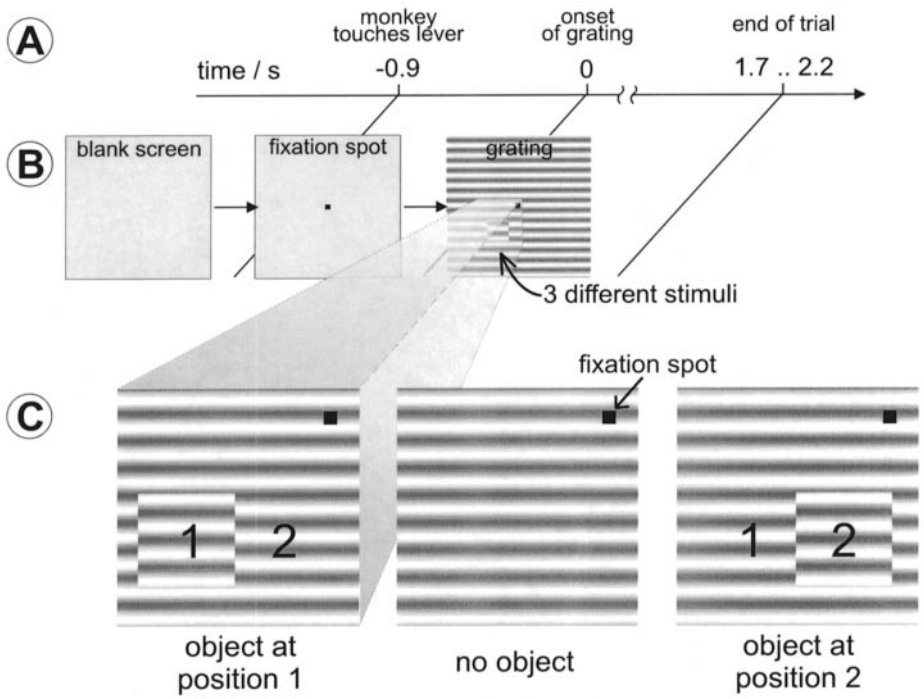

Figure 1. Time course of stimulus presentation and behavioral control of a single trial. (*A*) Succession of events. (*B*) Sequence of stimulation. (*C*) Enlargement of the stimulation area containing the object and the fixation spot (black square). Note that the object in positions 1 and 2 is mirrored at one of its vertical edges.

neurons, and in the two stimulus situations oscillations with reduced correlation. Hence, even though both experiments did not directly test the classical figure–ground situation, they came to related results suggesting that segregation is supported by decoupling the activities of an object from that of its background representation.

However, a recent investigation in monkey V1 seems to challenge the hypothesis of figure–ground segregation by decoupling (Lamme and Spekreijse, 1998). In this study, the relationship between the correlation of pair recordings and the perceptual organization of the scene was in many cases not consistent with the hypothesis of feature-linking-by-synchronization. In their experiments various scenes were presented, consisting of a figure on a background composed of similar texture elements. In particular, the strength of MUA cross-correlations between pairs of recording sites often were not significantly different, when the sites represented elements of the same scene segment compared to when they represented figure and ground. Consequently, the authors concluded that synchrony in V1 does not reflect the binding of features.

Our Investigation

In our present investigation we primarily wanted to clarify the seemingly contradictory results of coupling and decoupling among representations of two different segments of a scene, in particular the effect exerted by a contour defined by textures. Other, as yet uninvestigated, coupling mechanisms may play a role in figure–ground coding. They should become visible in the modulation of other types of coupling measures or in different frequency ranges. In our investigation we therefore analyzed several signal components and measures, including cross-correlation, coherence in the gamma (γ = 35–90 Hz) and low-frequency (1–20 Hz) ranges of multiple unit activity and local field potentials and time courses of spike rate modulations. Monkeys were shown a figure–ground stimulus consisting of object and background regions whose features were as identical as possible. We chose a grating texture of equal contrast, spatial frequency and orientation, in which the object was exclusively defined by an offset in the grating's spatial phase within a quadratic region. In contradiction to the conclusions of Lamme and Spekreijse (Lamme and Spekreijse, 1998), our results from V1 suggest that figure–ground segregation is supported by desynchronization. We demonstrate this by a systematic strong decoupling across the object's contour yielded by a substantial reduction in coherence of γ-LFPs between inside and outside of an object's representation in two monkeys. Additionally, an object-specific rate enhancement was present in one monkey, confirming previous observations partly (Lamme, 1995; Lamme *et al.*, 1998a,b, 1999). [Preliminary results of this investigation have been published as conference abstracts (Guettler *et al.*, 1997; Gail *et al.*, 1999).]

Materials and Methods

Visual Stimulation and Behavioural Task

Visual stimulation

Visual stimuli were applied using a 21-in. computer monitor with 98 Hz frame rate and 800 × 600 pixel resolution at a distance of 125 cm in front of the monkey, covering ±9.1° × 6.8° of the animal's visual field. The stimulus consisted of a sinusoidal grating extending over the whole screen. Within this area a square object was defined by a 2.75° × 2.75° part of the grating shifted in spatial phase (Fig. 1; grating luminance: 0.6–58.0 cd/m^2 ; Michelson contrast 98%; luminance of the homogenous gray screen and the surrounding walls were adjusted to the average luminance of the grating of 6 cd/m^2, using a logarithmic scale).

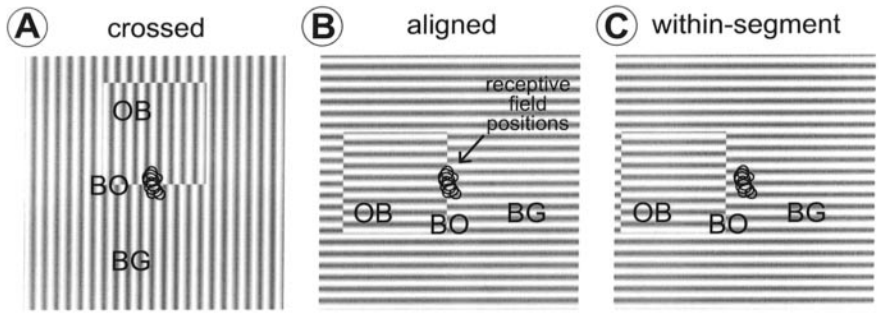

Figure 2. Three different arrangements of the classical receptive fields relative to figure and ground. Recordings were made by a linearly arranged array of seven μ-electrodes. (*A*) Receptive field array across the contour, (*B*) along the contour, (*C*) parallel to the contour, i.e. within a scene segment (average receptive field distance from the contour is the same as that of the outer receptive fields in *A*). Note that the object positions but not those of the receptive fields have been changed during the same recording session. OB, object; BO, figure–ground border; BG, background.

The spatial frequency of the grating was kept constant within each recording session while it could vary between sessions. We used frequencies of 1–5 cycles/deg, which guaranteed adequate activation at the recording eccentricities chosen in V1. Within blocks of trials the orientation of the grating was kept constant, but it was varied between blocks to allow for different arrangements of the classical receptive fields relative to the object (Fig. 2, and see below).

Time Course of Stimulus Presentation and Behavioural Control

The monkey fixated a green spot (6.5′ × 6.5′ visual angle; 39 cd/m^2), which appeared at the center of the screen when he indicated his readiness for the next trial by touching a lever (Fig. 1*A*,*B*). This fixation spot remained visible during the trial. The trial was ended immediately when the monkey released the lever or failed to keep fixation within 1.2° × 1.2° visual angle. Eye movements were controlled by an infrared camera system with 225 Hz frame rate and a resolution of 0.1°, developed in our group. Unless the trial was aborted early, the fixation spot dimmed to 23 cd/m^2 at the end of the trial. Subsequently the monkey had at most 0.65 s to react by releasing the lever. He was only rewarded with water or juice when he did not interrupt the trial early and managed to react to the dimming in time. These trials were the correct ones that were evaluated. The regular end of a trial was reached after a total of 2.6–3.1 s. This interval contained a 0.9 s prestimulus interval with a blank screen followed by the grating stimulus interval of random duration of 1.7 to 2.2 s (Fig. 1*A*,*B*). Trials were separated by a pause of ~2 s duration.

Preparation and Recording

Experiments were performed on two male rhesus monkeys (*Macaca mulatta*) aged 7 (monkey H) and 12 years (monkey S). Preparation and recording were carried out as reported elsewhere (Eckhorn *et al.*, 1993a; Frien *et al.*, 1994) in accordance with German laws of animal maintenance and experimentation and the guidelines published in the NIH *Guide for the Care and Use of Laboratory Animals* (NIH publication no. 86–23, revised 1987). In short, under deep barbiturate anesthesia three stainless-steel bolts were affixed to the skull for painless head fixation during the recording sessions, in addition to a stainless-steel chamber of 8 mm o.d. giving access to primary visual cortex (V1) through the intact dura. After a few days of recovery, recording sessions started. In each session seven linearly arranged, quartz-insulated, platinum–tungsten fiber-microelectrodes with 500 or 750 μm inter-electrode spacing (Eckhorn and Thomas, 1993) were inserted individually into the upper layers 2 and 3 of V1, and neural activities were recorded extracellularly in parallel from all electrodes.

Data Aquisition and Analysis

Data Aquisition

Two types of signals were extracted from the raw broad-band signal (1 Hz to 10 kHz). Multiple unit activity (MUA) was extracted by band-passing (1–10 kHz; 18 dB/oct), full-wave rectification and subsequent low-pass filtering (140 Hz; 18 dB/oct), yielding an amplitude-weighted measure of population spike activity near the electrode tip without rejecting low-amplitude spikes. The mean MUA level during prestimulus recording (blank gray screen with fixation spot) was subtracted from the following response epochs. Second, local field potentials (LFP) were obtained by band-passing from 1 to 120 Hz. Both analog signals (MUA, LFP) were sampled at a rate of 500 Hz.

Mapping of Classical Receptive-Fields

Position and extent of the classical receptive fields were measured with the RF-cinematogram method (Eckhorn *et al.*, 1993b). For this, a white spot of Gaussian luminance distribution changed its location pseudo-randomly every 30.6 ms on a hexagonal grid within a rectangular frame containing all pre-estimated receptive field positions. Cross-correlation between stimulus position and responses yields a time-resolved projection of the neuron's spatial response profile in visual space, i.e. the temporal development of the spatial aspects of the receptive field structure. To extract the receptive field position and extent, the temporal dynamics were ignored. Receptive field measures were obtained by averaging over the epoch of the strongest response (50–120 ms post-stimulus). This raw receptive field profile was spatially interpolated and the contour of the 71% level was considered the receptive field contour. Hence, its center of mass gives the receptive field center, the average diameter a measure for its size which is close to that obtained with the minimum response method (Barlow, 1972). In contrast to methods using a moving light bar as stimulus, this procedure avoids the uncertainty in reconstructing the receptive field position from the bar movement due to delay differences for stimulus movement directions with differences in response strength. Instead, a moving light bar of low velocity (1.5°/s) was used to obtain the orientation characteristics of the recording positions. Eccentricities of receptive field centers were parafoveally between 0.9° and 2.1° with extents varying from 0.2° to 0.6°. Corresponding LFP receptive fields were on average 30% larger in diameter (the sizes for MUA and LFP were determined with the same criteria and from the same raw recordings).

Classification of Receptive Field Positions

The visual stimulus consisted of a rectangular object defined by texture contrast. Simplifying the situation, we defined three classes of receptive field locations relative to the area of the object by grouping them with respect to the location of their receptive fields (Fig. 2). Each recording position belongs to either the object's surface (OB), the object's contour ('border': BO) or the background (BG). This classification was made on the basis of MUA receptive fields obtained by the RF-cinematogram method. Only channels with MUA of sufficient signal-to-noise ratio are considered in our analyses. Whenever the MUA receptive field contour at a given recording position intersects the object's border, it belongs to the contour representation (BO). Otherwise it is part of the object's surface

(OB) or the background (BG), depending on which side of the contour it lies.

PSTHs, Spectral Analysis and Coupling Measures

Different measures were calculated in our analyses in the temporal and spectral domains: peristimulus time histograms (PSTHs), power spectra, cross-correlation and coherence functions. To estimate the stimulus-locked components of the signals and their coupling strength, a shift-predictor (Perkel *et al.*, 1967) was calculated for power spectra and cross-correlation functions. Modulations of these measures due to different stimulus conditions were calculated for the stimulus specific portions of the responses, which means the pre-stimulus (baseline) level of each measure was subtracted before calculating relative changes. For comparability with previous work, modulations of cross-correlation coefficients were additionally calculated with subtraction of the shift-predictor (without subtracting the pre-stimulus correlation).

Except for PSTHs, a sliding-window technique was used with an epoch length of 128 ms and a shift of 32 ms. After windowing the data by a box car function, the mean value was subtracted for each epoch individually. For spectral measures, epochs were then multiplied by a Hamming window before calculating a fast Fourier transform (FFT).

Coherences were calculated across the number of trials with absolutely identical stimulation [Bartlett-smoothing (Glaser and Ruchkin, 1976)] and sorted with respect to different stimulus parameters such as object position or spatial phase of the grating. Additional averaging, e.g. across different spatial phases of the grating or across different recording positions, was performed on these coherence values. As for all other normalized measures, this was done with Fisher *Z*-transformed values.

The spectral resolution was restricted to 7.8 Hz due to the window length. Two frequency ranges were distinguished: the low-frequency range up to 20 Hz (bin 0: 0–4 Hz to bin 2: 12–20 Hz; note that for LFPs the lower band-pass limit is 1 Hz in our recordings) and the γ-range from 35 to 90 Hz (bin 5: 35–43 Hz to bin 11: 82–90 Hz). The latter range is determined by the typical stimulus-specific increase of the average signal power within this range and is separated from the low-frequency range by a gap of low signal power around 30 Hz.

Receptive Field Arrangements and Object-related Modulations

To compensate for possible dependencies on contrast polarity of the neural activation at single recording positions, we used three different absolute spatial phases of the grating and averaged data across these conditions. The spatial phases of the object and background areas were varied independently. As a consequence, in one third of the trials the phase difference between object and background was zero and therefore no object but a continuous grating was visible (Fig. 1*C*, center). With a phase difference and the object visible, it could appear at two positions mirrored at one edge (Fig. 1*C*). This ensured equal relative frequency for each recording position (not part of the contour representation) to be part of the object and the background representation while keeping the same distance to the contour. Variation of the spatial phases ensured on average locally identical stimulation in both conditions.

Comparison of the two conditions with different object positions allowed object-specific modulations to be extracted, as Lamme and colleagues did (Lamme, 1995). Comparison of the conditions with or without object allowed modulations specific for texture segmentation to be extracted.

To analyze data with respect to both kinds of modulation we made the relevant edge of the object, i.e. the one the object's position was mirrored at, intersect the linear array of receptive fields halfway. We call this condition the 'crossed' arrangement (Fig. 2*A*). Additionally, we used arrangements with all receptive fields lying at the object's contour ('aligned' arrangement; Fig. 2*B*) or parallel to it with the same offset as the outer receptive fields in the crossed arrangement had ('within-segment' arrangement; Fig. 2C).

Stimuli for different receptive field arrangements during the same recording session were presented blockwise, while variation of all other stimulus parameters was done pseudo-randomly within blocks of trials.

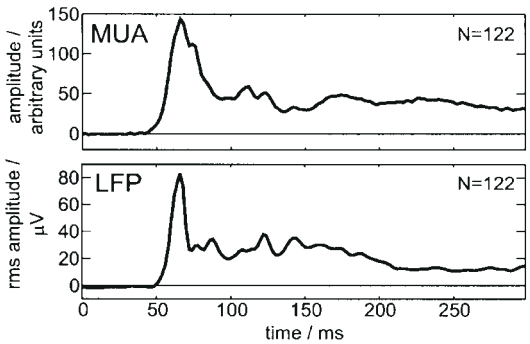

Figure 3. Average peristimulus time histograms (PSTHs) in response to the continuous grating stimulus pooled from both monkeys. The vigorous transient early responses and the sustained continuing activation of multiple unit activity (MUA) and local field potentials (LFP) were separated from the same raw data. They indicate that both types of signals were, on average, equally well driven by the grating stimuli (switched on at time zero). Note that we calculated root-mean-square values for LFP in this depiction.

Results

Analyzed Data

In 19 recording sessions data sets from 133 recording positions were obtained. After visual inspection and rejection of faulty recording positions (due to broken electrode tips and other artifacts) complete recordings from 54 of 56 positions (monkey H) and 68 of 77 positions (monkey S) were used for further analysis.

Pairwise coupling of neural responses was characterized by the coherence in the low-frequency and γ-range and cross-correlation coefficients at zero time lag (baseline or shift-predictor subtracted). The four coupling measures were calculated for MUA and LFP for the first five post-stimulus epochs in both monkeys.

We primarily addressed the question of reduced coupling between object and background representations, and for this condition LFP coherence in the γ-range is the only one of the determined coupling measures that shows this reduction at high significance in consecutive epochs. We therefore mainly present results on the basis of LFP γ-coherence, although we also compare other coupling measures.

Stimulus-related Modulation of Coherence: Within-segment Condition

Within the representation of the same scene segment (object, background or whole field) stimulation induced particularly high values of LFP coherence in the γ-range (35–90 Hz). Figure 4 shows the average temporal development of coherence during the first 254 ms post-stimulus when both recording sites are part of the object's surface representation (solid curve). During the early post-stimulus epoch (0–126 ms), LFP coherence is elevated within a broad spectral range compared to the pre-stimulus epoch (dotted curve). This stimulus-specific increase in LFP coherence is especially present above 30 Hz. With advancing time the range of elevation shrinks to a band of ~40–80 Hz. MUA shows on average very weak, stimulus-specific γ-coherence (Fig. 4), even though MUA is on average as vigorous in its early response and as sustained in its later response phases as LFP (Fig. 3). The pattern of coherence modulation in Figure 4 is identical when the same recording sites are part of the background representation and is almost the same with stimulation by the continuous grating (dashed curve).

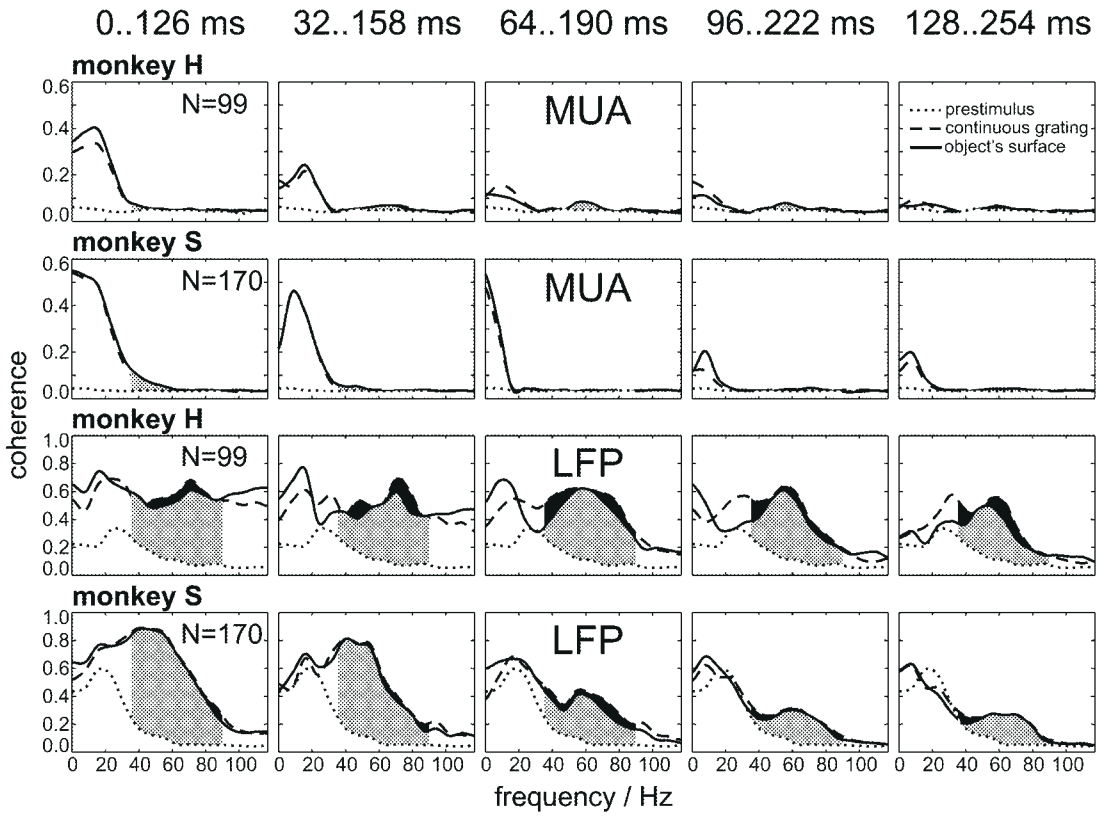

Figure 4. Post-stimulus temporal evolution of average MUA and LFP coherence in the within-segment condition (monkey H: $n=99$; monkey S: $n=170$). Coherence in positions at background representation are nearly identical to those at object representations (continuous lines) and therefore not shown. Pre-stimulus values are included in all diagrams for comparison (dotted lines). Shaded areas indicate the γ-range (35–90 Hz). Gray shading: difference between pre-stimulus and within-segment coherence. Black shading: difference between continuous grating (dashed lines) and within-segment condition. The broad-band increase in LFP-coherence directly after stimulus-onset declines in the lapse of time particularly at low frequencies, while LFP γ-coherence remains enhanced relative to prestimulus values. Note that the coherence for the condition of both receptive fields within the same segment compared to that of both at the continuous grating is very similar. Note also the different scales for MUA and LFP.

In principle, the within-segment condition can be analyzed in the crossed receptive field arrangement (Fig. 2*A*) as well as in the within-segment receptive field arrangement (Fig. 2*C*). In the latter condition, electrode pair distances range from 1 to 6 inter-electrode spacings (of 500 or 750 μm each). In the crossed receptive field arrangement, at most three receptive fields were lying at one side of the contour. This means that only recordings from distances of 1 or 2 electrode spacings contribute to averages in this condition. Nevertheless, the average time courses of coherence look qualitatively the same in both arrangements.

Stimulus-related Decoupling of γ-Activity Among Object and Background Representations

γ-Coherence

The coupling behaviour between neural populations of the object and background representations is different in the continuous compared to the figure–ground condition, which was investigated in the crossed receptive field arrangement (Fig. 2*A*). Figure 5*A* shows a clear decoupling effect indicated by a substantial decrease of LFP γ-coherence. Strongest relative reduction occurs in both monkeys nearly in the same post-stimulus epoch (around 180 ms). For monkey H, LFP γ-coherence across the object's border nearly drops to the pre-stimulus level in the interval 128–254 ms post-stimulus. This occurs simultaneously with the object-specific spike rate enhancement at the object's

Table 1
Test results (*P*-values) for the differences between the coupling strength (either coherence or cross-correlation) across the contour and the coupling strength in the situation with the continuous grating for identical receptive field positions

	Coherence		
	Epoch (ms)	1–20 Hz	35–90 Hz
MUA	0–126	0.392	0.458
	32–158	0.032	0.182
	64–190	0.014	0.275
	96–222	0.332	0.443
	128–256	0.0020	0.149
LFP	0–126	0.283	0.058
	32–158	0.441	0.0010*
	64–190	0.474	0.0000002**
	96–222	0.0053	0.0000007**
	128–256	0.244	0.0000002**
	Cross-correlation		
	Epoch (ms)	Minus baseline	Minus shift-predictor
MUA	0–126	0.318	0.149
	32–158	0.250	0.193
	64–190	0.027	0.017
	96–222	0.00029*	0.0023
	128–256	0.00031*	0.000011**

Wilcoxon rank-sum test, $n = 68$. Asterisks indicate levels of significance after Bonferoni correction: $*P_{eff} < 0.05$, $**P_{eff} < 0.01$. For details see text.

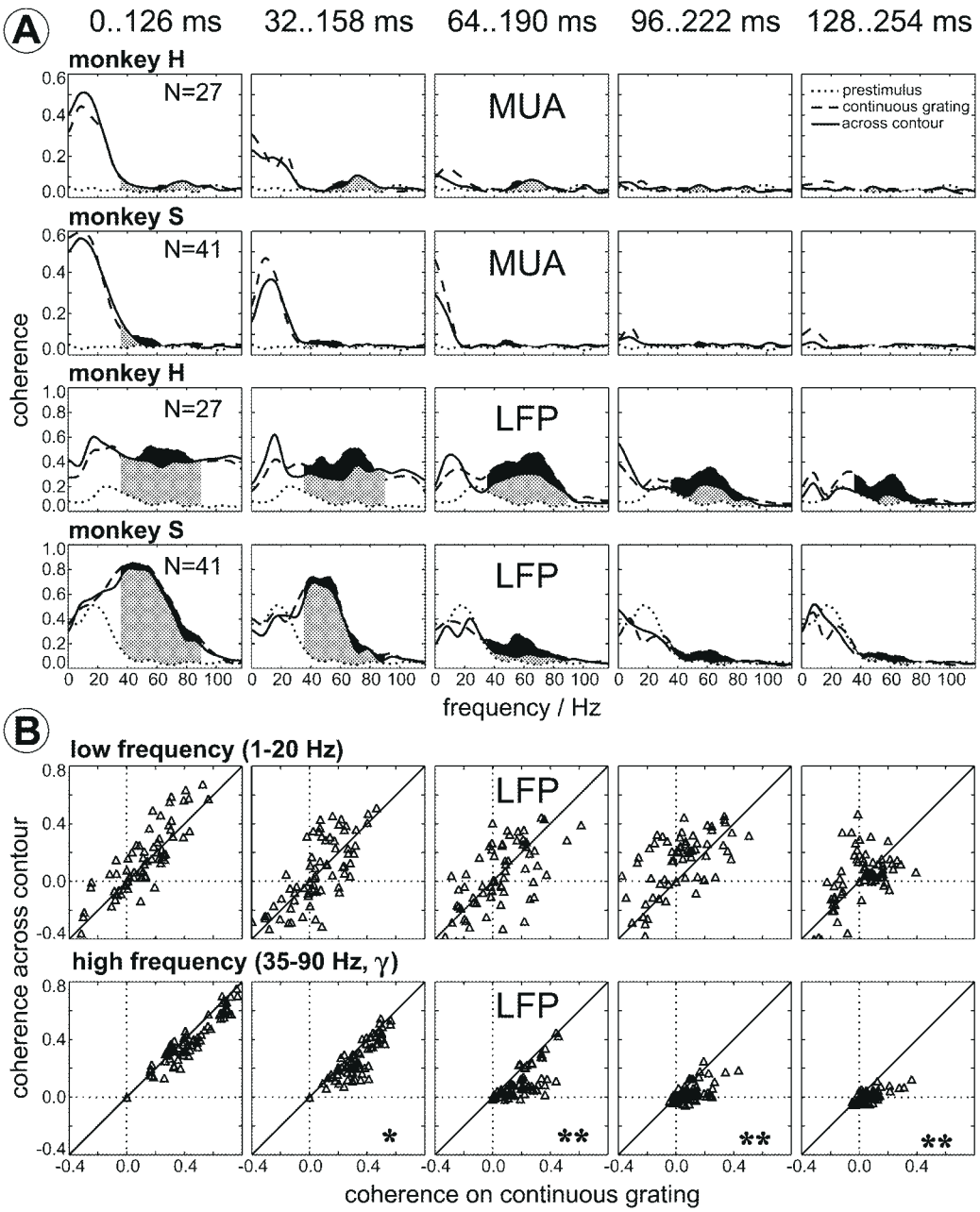

Figure 5. Post-stimulus temporal evolution of average MUA and LFP coherence in the across-contour condition (solid lines). (*A*) Average coherence for monkeys H ($n=27$) and S ($n=41$). Pre-stimulus values are included in all diagrams for comparison (dotted lines). Shaded areas indicate the γ-range (35–90 Hz). Gray shading: difference in coherence between pre-stimulus and across-contour conditions. Black shading indicates the difference between continuous grating (dashed lines) and across-contour conditions. Note the strong and broad-band increase in LFP coherence for both receptive field arrangements directly after stimulus-onset (particularly in monkey S). (*B*) Upper panels: comparison of low-frequency LFP coherence (1–20Hz) obtained with continuous grating (abscissa) and across-contour arrangement (ordinate); pooled data from both monkeys. Lower panels: comparison of LFP γ-coherence with continuous and across-contour arrangement. Note that the γ-frequency but not the low-frequency LFP coherence is highly significant reduced during the late three post-stimulus epochs in the crossed compared to the continuous condition.

surface representation in this monkey (not shown). In monkey S the dissociation of the coupling on the continuous grating versus the coupling across the contour reaches its maximum ~30 ms earlier than in monkey H (96–222 ms post-stimulus).

During the early post-stimulus epochs (0–126 ms), relative differences in γ-coherence between the continuous and the figure–ground condition are small (H: 15%; S: 10%) and become large (H: 80%; S: 78%) during the later response epochs (H: 128–254 ms; S: 96–222 ms), which indicates that the stimulus-locked components of the early responses do not show contour-related coherence reduction (see Discussion).

As data from both monkeys show qualitatively the same effects, we merged them (Fig. 5*B*, lower panels). Differences between stimulus conditions were tested separately for each coupling measure and epoch with the Wilcoxon rank-sum test. To compensate for error accumulation due to multiple testing, the alpha criterion was conservatively corrected with a factor of 40 (4 different coupling measures × 5 post-stimulus epochs × 2

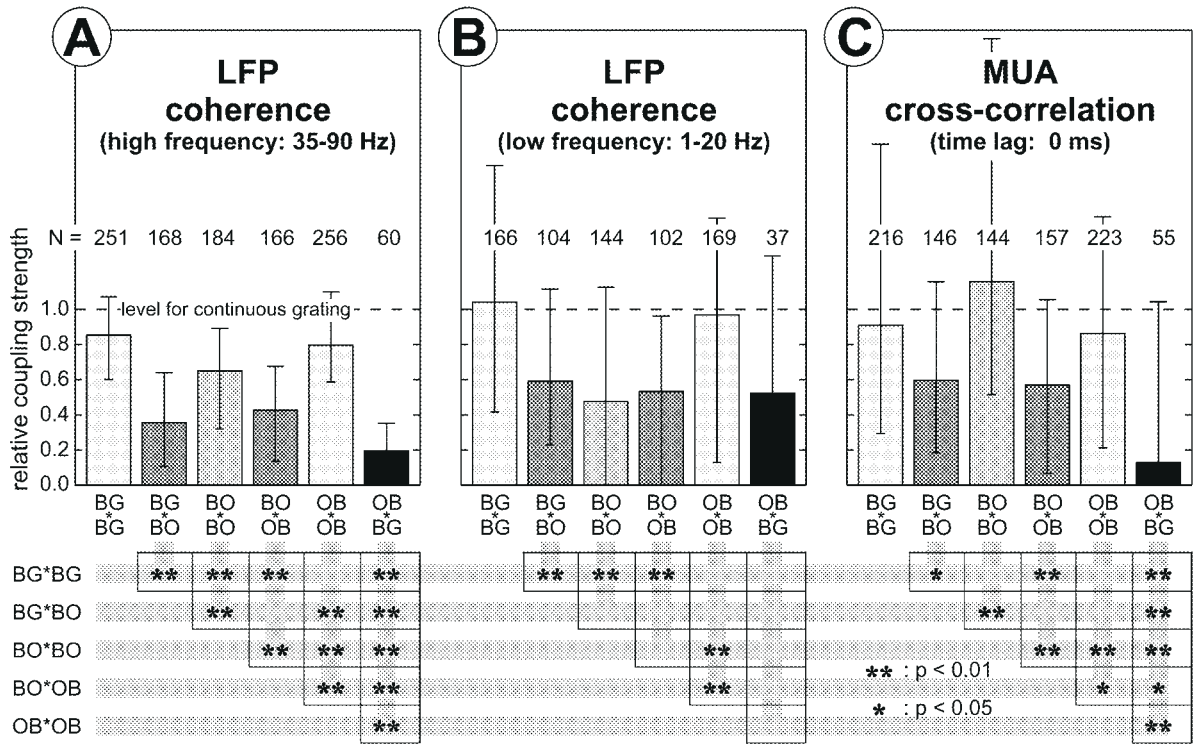

Figure 6. Coupling strength for different measures and different positions of the receptive fields relative to the figure–ground contour normalized to the values obtained with the continuous grating. The bar heights represent the median ratio of coupling strength for the signal components in response to the figure–ground stimulus and the continuous grating (error bars indicate quartiles). Note that for coherence the baseline and for cross-correlations the shift-predictor was subtracted and negative values can occur. Therefore only those recording pairs were taken into account that showed positive coupling values in the continuous grating condition (their numbers *n* are plotted above each bar). The total numbers of recorded pairs for the different conditions are: 269 (BG*BG, OB*OB), 173 (BG*BO, BO*OB), 197 (BO*BO) and 68 (OB*BG). Data is merged from both monkeys and for each monkey we took the optimal post-stimulus epoch: 96–222ms (S) and 128–254ms (H). The matrices in the lower panel show corrected levels of significance for Wilcoxon rank-sum tests on differences between the coupling values for different receptive field locations. (*A*) LFP γ-coherence. Due to the introduction of the figure–ground contour, within-segment situations (BG*BG and OB*OB) have slightly reduced LFP γ-coherence (~20%), while across-contour situations (BG*OB) show strong reductions in LFP γ-coherence (80%). Intermediate reductions were obtained between border and one of the segments (BG*BO and BO*OB). (*B*) LFP low-frequency coherence shows high variance (large error bars). Note that the number of recording pairs with positive coupling values is much lower than for LFP γ-coherence. (C) MUA cross-correlation results coarsly resemble those for LFP γ-coherences, but at much higher variance.

signal types: MUA, LFP) due to Bonferoni, i.e. an effective $\alpha = 0.01$ was tested with $\alpha' = 0.00025$. The main results of these tests are summarized in Table 1. The reduction in stimulus-specific LFP γ-coherence ('stimulus specific' refers to the fact that the estimate for non-specific coherence during the prestimulus interval has been subtracted, cf. Materials and Methods) is highly significant for the three later response epochs (64–254 ms post-stimulus), while this is not the case for the first two epochs (0–158 ms). There are no significant differences in coherence during any stimulus epoch for the low-frequency band, neither with LFP (Table 1 and Fig. 5*B*, upper panels) nor with MUA, indicating that there are no consistent changes in coherence for low-frequency components among figure and background positions.

MUA Cross-correlation

MUA cross-correlation analysis was calculated for comparison with previous work (Lamme and Spekreijse, 1998). It reveals the same tendency for the reduction in coupling strength among figure and background positions as seen with γ-coherence of LFP, but less clearly (Table 1). The reduction in cross-correlation coefficient does not become highly significant in any of the post-stimulus epochs when the pre-stimulus correlation is subtracted (while the shift-predictor is not subtracted), and it does become highly significant only during a single epoch (128–254 ms) when the shift-predictor is subtracted (while the pre-stimulus correlation is not subtracted).

Reduction in γ-Coherence Near the Contour Representation: Control Experiments

The decoupling across the object's contour would not be of greater interest if decoupling was induced by the contour equally well among within-segment and among across-contour positions. We therefore used the alternative within-segment receptive field arrangement by rotating the figure–ground stimulus while keeping the identical recording sites as control (Fig. 2*C*). In this condition approximately the same distance of the contour to the receptive fields of both sides was realized as in the crossed receptive field arrangement. A major difference was the collocation of the receptive fields lying in the crossed-condition on either side of the contour and in the within-segment arrangement on the same side. Here, differing from Figure 4, data of the within-segment arrangement only includes those electrode pairs that also contribute to data in the crossed arrangement ($n = 34$ for monkey S; $n = 14$ for monkey H), which are those positions in the crossed arrangement not lying on the object's contour.

In this control condition the reduction in γ-coherence is relatively low (<20%) compared to the case when the receptive fields lie on different sides of the contour (80%; see Fig. 6). This demonstrates that decoupling across the contour representation

is due to the intersecting character of the contour and not due to its vicinity alone (see Discussion).

γ-Power and γ-Coherence Along the Contour Representation

In search of potential mechanisms of decoupling across the contour, the coupling strength at the contour itself was analyzed. This revealed lower values of LFP γ-coherence compared to the continuous grating and the within-segment condition during the post-stimulus epochs between 64 and 256 ms. Although the stimulus-related reduction is not as drastic as across the contour it is nevertheless remarkable (~40%). However, stimulus-specific LFP γ-amplitude density is also decreased at representations of the contour compared to that of the continuous grating: max. 35% in monkey H and max. 40% in monkey S (52–60 Hz; 64–190 ms).

Comparison of Different Coupling Measures in All Combinations of Relative Receptive Field Positions

To summarize the pattern of stimulus-specific modulations in coupling, Figure 6 compares relative values of different measures in all combinations of relative receptive field locations. Since pairs of recording sites with different average distances are pooled for the different groups of relative receptive field locations (OB*OB, OB*BO, etc.) we normalized the coupling values for each electrode pair to the corresponding value in the continuous grating condition before averaging. This enables direct comparison of stimulus-related modulations for the different situations. Baseline or shift-predictor values were subtracted. For Figure 6 we only consider those recording pairs showing positive coupling values in the continuous grating condition after this subtraction, because we wanted to know the modulations which are specifically due to insertion of the object. In addition, results in this compilation (Fig. 6) are calculated in the optimal time interval for each monkey, i.e. 128–254 ms for monkey H and 96–222 ms for monkey S.

In Figure 6*A* four levels of LFP γ-coherence can be distinguished. Firstly, the strongest coupling is present between groups of neurons that represent the same scene segment when both receptive fields lie on the object's surface (OB*OB) or on the background (BG*BG). Secondly, in the situation with both receptive fields on the object's border (BO*BO), coherence is lower compared to the within-segment condition (~65% compared to continuous grating). Thirdly, an intermediate coupling strength is observed for pair recordings where one receptive field belongs to the contour and the other to the object's surface (BO*OB) or to the background (BG*BO). Fourthly, and most importantly for the present investigation, the weakest coupling (strongest decoupling) is present when one receptive field lies on the object's surface and the other on the background (OB*BG). Except the comparisons BG*BG versus OB*OB and BG*BO versus BO*OB all differences in LFP γ-coherence are highly significant (Wilcoxon, $P < 0.01$; see significance matrix in Fig. 6).

For low-frequency LFP many recording pairs do not show a stimulus-specific increase in coupling at all, as one can already see from Figure 5*B*. There are significant differences in coupling modulations only between locations including the object's border versus those lying completely inside or outside the object representation. For figure–ground segregation the across-contour condition (OB*BG) is relevant, but this shows no significant differences with respect to all other receptive field locations (right column of significance matrix in Fig. 6*B*). The modulations of MUA cross-correlations (Fig. 6*C*) coarsely resemble those of LFP γ-coherences, but at much higher variance (indicated by the large error bars) and therefore with significant results only in fewer combinations of recording positions. However, the reduction in coupling among figure and ground locations are highly significant compared to most of the other combinations.

Stimulus-related Modulations in Spike Rate

Our figure–ground stimulus design has a lot in common with that of previous studies (Lamme, 1995; Zipser *et al.*, 1996; Lamme *et al.*, 1998a,b) which demonstrated a late increase in spike population activity (MUA) within the representational area of an object's surface compared to that of the background in V1 of awake monkeys. Such object-specific modulations in MUA are also clearly present in our monkey H between 150 and 260 ms post-stimulus. However, in monkey S the same analysis does not reveal any significant difference (data not shown).

Discussion

Main Results

We demonstrate that the coherence of late LFP γ-components is strongly and significantly reduced across a contour's representation. This effect is also visible in MUA cross-correlations during late epochs but at much higher variance. However, γ-coupling is on average almost not influenced during the early response phase, when stimulus-locked components dominate, and this is also true for low-frequency coherences during the entire response epoch (LFP and MUA). Hence, our results suggest that the decoupling of fast signal components is particularly suitable for supporting figure–ground segregation.

Contradictory Results from Other Work?

While our data reliably demonstrate substantial reduction of coupling across the representation of a texture contour compared to the continuous texture, this was not the case in the work of Lamme and Spekreijse (Lamme and Spekreijse, 1998) under similar stimulus conditions. In their experiment decoupling across contours is present in only a fraction of visual situations. This led them to the conclusion that scene segmentation is not supported by decoupling of signals at the contour representation. How can these differences be explained?

While we obtained our clearest results on the basis of LFPs, those of Lamme and Spekreijse are based on MUA. Evaluation of our calculations of MUA coherence showed no effect at all, while cross-correlations revealed highly significant modulations only during a short epoch if stimulus-locked components were subtracted (without subtraction of baseline correlations). However, if baseline correlations were subtracted (without subtraction of the shift-predictor) no significant differences in modulation were found. This means that MUA data is much less reliable in this task than LFP (Table 1), even though both types of signal components were extracted from the same raw data. In other words, the results by Lamme and Spekreijse are not really contradictory to ours, but differences are probably introduced by our use of LFPs, which seem to be more sensitive for effects of synchronization in visual cortex than MUA. However, our conclusion challenges that of Lamme and Spekreijse, because the reduction in LFP coherence in our results is highly significant and reliable and is taken therefore as an indication that decoupling of high-frequency components seems suitable for coding scene segmentation.

LFP versus MUA Recordings

LFP provides a conservative measure for the effect of coherence reduction in the present experimental situation, because LFP is volume conducted over larger areas than spike activities (half height decline of about 500 and 50 μm respectively). This is also visible in our receptive field measurements which have on average 30% larger diameters with LFP compared to MUA (same raw data; same criterion). Volume conduction counteracts the effect of coherence reduction across the contour representation the closer the recording positions are to the contour, because decoupled activity from the other side of the contour representation is partly picked up.

Several properties of MUA are disadvantageous for the evaluation of the coupling phenomena analyzed here. Firstly, MUA contains strong broad-band stochastic power, including the γ-range, that is not correlated with visual stimulation. Secondly, these broad-band components are only correlated among recording positions within a short distance range in V1 (Koenig *et al.*, 1995). Both properties result in MUA coupling values declining much faster to noise level with increasing cortical distance than values of LFP coupling. Hence, at many pair recording positions MUA cross-correlation and coherence are at noise level, which means they do not relevantly contribute to grand averages. This argumentation is supported by comparison of LFP and MUA results obtained from the same raw data in our present investigation. LFP shows reliable coupling, while MUA does not.

The higher sensitivity of LFPs for cortical coupling is probably inherent in their generation. They reflect the superimposed postsynaptic activities of thousands of neurons where the independent stochastic activities are canceled out while the coordinated fluctuations (the synchronized components) survive (Mitzdorf, 1985). Thus, LFPs are well suited for analyses of interactions among spatially well separated populations of cooperating neurons (>500 μm: half decline of volume conducted field). In summary, results similar to ours may have been obtained if Lamme and Spekreijse had used LFP for their analyses.

Reduction of LFP γ-Coherence Across the Contour is not a Result of a General Reduction in γ-Coherence

If the presence of a contour generally reduced coupling strength on either side of its representation (and not only across it), segregation by decoupling would not work. However, our data demonstrate that this is not the case. When the recording positions (which were kept constant over all stimulus situations; Fig. 2) were all at the object's or the background's representation in parallel to the contour, the appearance of the object and its contour induced only small reductions in γ-coherence of LFP (20%) compared to the situation with one receptive field inside and the other outside the object (80%). The small coherence reductions, due to the neighborhood of the contour, parallels a decrease of γ-power in this situation, but our data give no hint whether and how these effects are related. Anyhow, the strong reduction in γ-coherence across the contour cannot be explained by the small effects parallel to it because the signals at both sides of the contour's representation largely keep their within-segment coherence.

Not Only γ-Oscillations but also Non-rhythmic γ-Activity is Decoupled Across the Contour Representation

In our recordings the strong reductions in LFP coherence across the contour representation are present over the entire γ-range (35–90 Hz), independent of whether the signals are oscillatory or non-rhythmic. This indicates that the mechanisms of decoupling do not operate selectively on rhythmic signals. In our LFP data always a mixture of rhythmic and stochastic components is present (the former characterized by a spectral peak) with different relative contributions depending on the monkey and the post-stimulus epoch. However, these changing contributions of fast oscillations to γ-activity do not influence the strength of decoupling. This is important because many visual stimuli do not induce γ-oscillations but cause a shift in spectral content from dominating low frequencies before stimulation, resembling an alpha EEG, to broad-band γ-components (Eckhorn *et al.*, 1993a; Frien *et al.*, 1994; Juergens *et al.*, 1999), according to a desynchronized EEG (Vijn *et al.*, 1991). As the stimulus-locked LFP components of the fast response at all frequencies and the later stimulus-induced components in the low-frequency range (1–20 Hz; not phase-locked to stimulus-onset) are not decoupled by the introduction of a contour, we assume it is the stimulus-induced γ-activity of the later response that is suitable for supporting figure–ground segregation. Probably the same neural mechanism of lateral signal decoupling is operative for rhythmic and non-rhythmic activity, and in addition, specifically influences the high- but not the low-frequency components. However, for a generalization of our assumptions a broad variety of scenes has to be tested in this respect in future work.

Coherence Reduction is Probably due to Blocking of Lateral Coupling Connections and not to Feedback from Higher Visual Areas

Strong coherence reduction (80%) is present among receptive field positions directly adjacent to either sides of the contour but not for pair positions at the same distance from the contour on a single side. As the receptive fields of V1 neurons are much smaller than those of neurons projecting back from V2, and in particular from V4, TE and TEO (Rockland and Drash, 1996), one would not expect such precisely confined decoupling driven by back-projections representing larger receptive fields. Hence, the spatial confinement of the step in coherence to the contour representation cannot be explained by decoupling actions from higher centers.

Instead, converging feed-forward connections from V1 to these higher visual areas establish the receptive field properties of their target cells, which may substantially be driven by the coherent signal components of their inputs (e.g. synchronized γ-oscillations). Hence, the back-projection will carry just these coherent components, resulting in correlations of V1 activities with signals of neurons that have overlapping receptive fields in the back-projecting visual areas (Eckhorn *et al.*, 1990; Engel *et al.*, 1991b; Frien *et al.*, 1994). The back-projection is therefore more likely to enhance coherent components in V1 across the broad regions of the receptive fields of higher areas than exerting a spatially confined reduction at the contour. In summary, it is probable that the lateral connections within V1 become disabled at positions of contour representations. The mechanism of decoupling cannot, however, be discovered from our present data.

No Coherence Reduction of Stimulus-locked Components at any Frequency

We call 'stimulus-locked' those signal components that are phase-locked to stimulus onset. They are extracted from the raw signal by stimulus-triggered averaging (via shift-predictor) and gain their prominent power from the short delay transient

response. In the present investigation inspection of coherence of stimulus-locked components among inside and outside representations of the object revealed no significant difference after insertion of the contour – neither in the low-frequency nor in the γ-range (even though strong stimulus-locked γ-components are present; Fig. 5). This again indicates that coherence reduction in stimulus-induced γ-activity is probably due to the blockade of lateral V1 connections by contour representations. Segregation based on differences in stimulus-locked signals at figure and ground representations in V1 would be extremely fast. A recent paper on figure–ground effects with texture stimuli discusses this possibility (Lamme *et al.*, 1999). It is shown that the fast stimulus-locked components evoked by the texture elements and texture-definded contours are not capable of supporting segregation between figure and ground, but a late increase in spike rate beginning 100 ms after stimulus onset is. The occurrence of this object-specific component corresponds temporally to the epoch where we find significant reduction of γ-coherence across the figure–ground contour. As this late γ-activation is not phase-locked to stimulus onset, it suggests, in correspondence to the results of Lamme and Spekreijse, that contributions to figure–ground segregation may well be supported by signal components that are not strongly driven by the stimulus but are considerably influenced by intrinsic mechanisms: the object-specific increase in the late spike rate is possibly influenced by top-down effects (Lamme *et al.*, 1998a,b) and the decoupling of late γ-activity by the lateral cortical network.

Relevance of Receptive Field Properties for Figure–Ground Segregation by Decoupling

In our analysis, we concentrate exclusively on the positions of the receptive fields and do not include other tuning properties like orientation preferences. This is done because the total number of recording positions (n = 122) is not sufficient for selecting enough cases with similar tuning at each side of the contour in order to make convincing statistical comparisons. However, we argue that perceived figure–ground contrast defined by textures is mainly based on the relative positions of local features at contours, and less, for example, by the local orientation of texture elements. Hence, if figure–ground segregation is based on γ-decoupling across contour representations, our results should not strongly depend on the local coding properties of the participating neural populations. This has not been analyzed to date.

However, some indirect hints on how neurons with different orientation preference contribute to the effects analyzed here are given by a recent work in which the same continuous grating has been used (Frien and Eckhorn, 1999). γ-Frequency, but not low-frequency, MUA coherence in V1 of awake monkeys is shown to be the stronger the more similar the orientation preferences are, and the better the grating stimulates the neurons (which is the case when the grating's orientation matches that of the receptive fields). But coupling is reliably present even among recording pairs with perpendicular orientation preferences, if the orientation of the stimulus activates both populations simultaneously. This means that positions with different orientation preferences and suboptimal match to the stimulus orientation also participate reliably in γ-coupling. Therefore, in our LFP recordings the populations matching the grating's orientation are likely to have contributed the dominant components to the high γ-coherence during stimulation, while positions with suboptimal match contribute less. However, populations not participating in this task may contaminate the LFP by their unrelated components of maintained activity which reduce coherence nonspecifically. In conclusion, the LFP coherence reduction in our present investigation is a conservative measure, which means we would expect higher coherence, and correspondingly larger coherence reductions, if we selected pair recordings with orientation preferences matching that of the grating.

We want to note that for the present work the orientation of the grating and the positions of the receptive fields were generally not changed with changes from object to continuous background presentations. This ensured that the same populations of neurons contribute to coherence with and without intersection by the contour.

Conclusions and Perspectives

Our experiment allows comparison of several coding aspects of object representation in monkey V1 in parallel. Contour- and surface-specific modulations of spike rate and γ-coherence of LFP show reliable characteristics appropriate for supporting figure–ground segregation, and thus, object coding. They probably reflect complementary mechanisms rather than being redundant. While spike rate enhancement at an object's surface representation in V1 is meant to be driven by top-down influences (Lamme *et al.*, 1998a,b), we assume that the decoupling effects among representations of both sides of a contour shown by us is a property of the lateral network in V1. The potential contributions of V1 to object coding are surely not sufficient for unique scene segmentation and object specification, particularly for complex scenes containing multiple objects. Apparently, additional visual structures and possibly other mechanisms are involved. In addition, future research should test whether reduction of high-frequency coherence is specific for a broad variety of visual situations. As figure–ground segregation may be supported by attentional mechanisms as early as in V1 (Roelfsema *et al.*, 1998; Vidyasagar, 1998), it would be interesting to study the combined action of rate enhancement at the surface representation of an attended object, as reported in recent work, and the γ-decoupling across its contour representation, as observed in our investigation.

Notes

Support by DFG to the research group 'Dynamics of Cognitive Representation' Ro529/12–1 to R.E. is greatly acknowledged. We also thank Professor R. Bauer and Michael Niessing for help in experiments, U. Thomas, W. Gerber and A. Rentzos for their expert support in experimental techniques, and two anonymous referees for their particularly constructive suggestions that helped to improve our manuscript considerably.

Address correspondence to Reinhard Eckhorn, Philipps-University, Physics Department, Neurophysics Group, Renthof 7, D-35032 Marburg, Germany. Email: reinhard.eckhorn@physik.uni-marburg.de.

References

Barlow HB (1972) Single units and sensation: a neuron doctrine for perceptual psychology? Perception 1:371–394.

Boucart M (1999) The neuroscience of perceptual integration. Hove: Psychology Press.

Brosch M, Bauer R, Eckhorn R (1997) Stimulus-dependent modulations of correlated high-frequency oscillations in cat visual cortex. Cereb Cortex 7:70–76.

Eckhorn R (1999) Neural mechanisms of visual feature binding investigated with microelectrodes and models. Visl Cogn 6:231–265.

Eckhorn R, Thomas U (1993) A new method for the insertion of multiple microprobes into neural and muscular tissue, including fiber electrodes, fine wires, needles and microsensors. J Neurosci Methods 49:175–179.

Eckhorn R, Bauer R, Jordan W, Brosch M, Kruse W, Munk M, Reitboeck HJ

(1988) Coherent oscillations: a mechanism of feature linking in the visual cortex? Biol Cybern 60:121–130.
Eckhorn R, Frien A, Bauer R, Woelbern T, Kehr H (1993a) High frequency (60–90 Hz) oscillations in primary visual cortex of awake monkey. NeuroReport 4:243–246.
Eckhorn R, Krause F, Nelson JI (1993b) The RF-cinematogram. Biol Cybern 69:37–55.
Eckhorn R, Reitboeck HJ, Arndt M, Dicke P (1990) Feature linking via synchronization among distributed assemblies: simulations of results from cat visual cortex. Neural Comput 2:293–307.
Engel AK, Koenig P, Singer W (1991a) Direct physiological evidence for scene segmentation by temporal coding. Proc Natl Acad Sci USA 88:9136–9140.
Engel AK, Kreiter AK, Koenig P, Singer W (1991b) Synchronization of oscillatory neuronal responses between striate and extrastriate visual cortical areas of the cat. Proc Natl Acad Sci USA 88:6048–6052.
Erb M, Aertsen A (1993) Dynamics of activity in biology-oriented neural network models: Stability at low firing rates. In: Brain theory — spatio-temporal aspects of brain function (Aertsen A, ed.), pp. 201–223. Amsterdam: Elsevier.
Frien A, Eckhorn R (2000) Functional coupling shows stronger stimulus dependency for fast oscillations than for low frequency components in striate cortex of awake monkey. Eur J Neurosci 12:1466–1478.
Frien A, Eckhorn R, Bauer R, Woelbern T, Kehr H (1994) Stimulus-specific fast oscillations at zero phase between visual areas V1 and V2 of awake monkey. NeuroReport 5:2273–2277.
Fukushima K (1980) Neocognitron: a self-organizing neural network model for a mechanism of pattern recognition unaffected by shift in position. Biol Cybern 36:193–202.
Gail A, Brinksmeyer HJ, Eckhorn R (1999) Different possible contributions of striate cortex activity to visual object representation in awake monkey. In: Proceedings of the 27th Göttingen Neurobiology Conference II (Elsner N, Eysel U, eds), p. 487. Stuttgart: Georg Thieme.
Glaser EM, Ruchkin DS (1976) Principles of neurobiological signal analysis. New York: Academic Press.
Gray CM (1999) The temporal correlation hypothesis of visual feature integration: still alive and well. Neuron 24:31–47.
Gray CM, Koenig P, Engel AK, Singer W (1989) Oscillatory responses in cat visual cortex exhibit inter-columnar synchronisation which reflects global stimulus properties. Nature 338:334–337.
Grossberg S, Pessoa L (1998) Texture segregation, surface representation and figure–ground separation. Vis Res 38:2657–2684.
Guettler A, Eckhorn R, Juergens E, Frien A (1997) Neural correlation contrast in visual cortex of monkey changes with stimulus contrast across an object-background-border. In: Proceedings of the 25th Göttingen Neurobiology Conference II (Elsner N, Waessle H, eds), p. 551. Stuttgart: Georg Thieme.
Horn D, Sagi D, Usher M (1991) Segmentation, binding, and illusory conjunctions. Neural Comput 3:510–525.
Juergens E, Guettler A, Eckhorn R (1999) Visual stimulation elicits locked and induced gamma oscillations in monkey intracortical- and EEG-potentials, but not in human EEG. Exp Brain Res 129:247–259.
Koenig P, Engel AK, Singer W (1995). Relation between oscillatory activity and long-range synchronization in cat visual cortex. Proc Natl Acad Sci USA 92:290–294.
Koffka K (1935) Principles of Gestalt psychology. NewYork: Harcourt.
Kreiter AK, Singer W (1992) Oscillatory neuronal responses in the visual cortex of the awake macaque monkey. Eur J Neurosci 4:369–375.
Kreiter A, Singer W (1996) Stimulus-dependent synchronization of neural responses in the visual cortex of the awake macaque monkey. J Neurosci 16:2381–2396.
Lamme VAF (1995) The neurophysiology of figure–ground segregation in primary visual cortex. J Neurosci 15:1605–1615.
Lamme VAF, Spekreijse H (1998) Neuronal synchrony does not represent texture segregation. Nature 396:362–366.
Lamme VAF, Supèr H, Spekreijse H (1998a) Feedforward, horizontal, and feedback interactions in visual cortical processing. Curr Opin Neurobiol 8:529–535.
Lamme VAF, Zipser K, Spekreijse H (1998b) Figure–ground activity in primary visual cortex is suppressed by anesthesia. Proc Natl Acad Sci USA 95:3263–3268.
Lamme VAF, Rodriguez-Rodriguez V, Spekreijse H (1999) Separate processing dynamics for texture elements, boundaries and surfaces in primary visual cortex of the macaque monkey. Cereb Cortex 9:406–413.
Mitzdorf U (1985) Current source-density method and application in cat cerebral cortex: Investigation of evoked potentials and EEG phenomena. Physiol Rev 65:37–100.
Palm G (1982) Neural assemblies. An alternative approach to artificial intelligence. Berlin: Springer Verlag.
Perkel DH, Gerstein GL, Moore GP (1967) Neuronal spike trains and stochastic point processes. Biophys J 7:420–440.
Rockland KS, Drash GW (1996) Collateralized divergent feedback connections that target multiple cortical areas. J Comp Neurol 373:529–548.
Roelfsema PR, Engel AK, Koenig P, Singer W (1996) The role of neuronal synchronization in response selection: a biological plausible theory of structured representations in the visual cortex. J Cogn Neurosci 8:603–625.
Roelfsema PR, Lamme VAF, Spekreijse H (1998) Object-based attention in the primary visual cortex of the macaque monkey. Nature 395:376–381.
Stoecker M, Reitboeck HJ, Eckhorn R (1996) A neural network for scene segmentation by temporal coding. Neurocomputing 11:123–134.
Vidyasagar TR (1998) Gating of neuronal responses in macaque primary visual cortex by an attentional spotlight. NeuroReport 9:1947–1952.
Vijn PCM, van Dijk BW, Spekreijse H (1991) Visual stimulation reduces EEG activity in man. Brain Res 550:49–53.
Wertheimer M (1923) Untersuchungen zur Lehre von der Gestalt: II. Psychol Forsch 4:301–350.
Zipser K, Lamme VAF, Schiller PH (1996) Contextual modulation in primary visual cortex. J Neurosci 16:7376–7389.